CHAPTER TWO

An Introduction to the Rheology of Polymeric Liquids

2.1 BACKGROUND

The establishment around 1930 of the field of rheology, the study of the deformation and flow of materials, was motivated by interest in the strange flow phenomena exhibited by polymeric liquids. A viscosity that depends upon the flow rate, liquids that "spring back" after a sudden deformation and liquids that climb from a free surface upward into a pipe are some examples of unusual flow behavior not associated with Newtonian liquids. Rheology generally excludes the study of low molecular weight liquids, mineral oil, for example, as it has been accepted that the flow of these liquids can been successfully described in every case by the Newtonian model. Bird et al. [1] placed a rough upper limit on Newtonian behavior at a molecular weight of 1000 kg/kmol. However, within elastohydrodynamics it has long been recognized that the Newtonian assumption must fail at very high pressures and shear stress in the conjunction of the concentrated contacts described in the previous chapter. At typical pressures of 1–2 GPa, the viscosity may be 10^9 Pa·s and the shear rate within the film may be 10^3 s^{-1}. Thin elastohydrodynamic films of much less than one micron thickness are very effective at removing the heat of viscous dissipation. Then for an isothermally sheared Newtonian liquid, the resulting shear stress of 10^3 GPa would easily exceed the strength of the strongest metals. Since sliding concentrated contacts operate successfully for years, with friction coefficients less than 0.1, lubricated by mineral oils of average molecular weight of about only 300 kg/kmol, some substantial departure from the Newtonian idealization must be occurring. Non-Newtonian flow in simple liquids, that is, branched alkanes, has been observed in exciting new results from nonequilibrium molecular dynamics simulations [2].

High Pressure Rheology for Quantitative Elastohydrodynamics.
DOI: https://doi.org/10.1016/B978-0-444-64156-4.00002-7

These simulations and experiments in pressurized rheometers support the notion that the nonlinear aspects of the shear behavior of polymers, in the form of shear-thinning and normal stress differences, can be observed in simple liquids as well provided that the shear stress is sufficiently large. Large shear stresses can be generated in thin compressed films of low molecular weight liquids.

Rheology can also been described as the search for the *constitutive equations* relating the stress to the deformation in a particular polymeric material. In this respect the field is incomplete; a constitutive equation can be written that is accurate over a limited range of kinematics only and part of the skill required in the application of rheology to practical problems is the recognition of which equation is appropriate for the present situation. Real flow problems are often so complex that the deformations cannot be known accurately without a priori knowledge of the constitutive relation. In order to test constitutive models and to provide rheological property data for their implementation, experiments are devised to produce flow kinematics that are simple and completely known. The apparatus for such experiments is a *rheometer*. If viscosity is the only property being measured, the apparatus is a *viscometer* even when measuring the shear dependence.

The materials studied by rheologists include neat liquid polymers (polymer melts), polymers dissolved in low molecular weight liquids (polymer solutions), suspensions of a second immiscible liquid phase, suspensions of solid particles or gas, and semisolid materials displaying a yield stress. Here, because of the application to lubrication only the liquid polymer and polymer solution behavior is addressed. Some lessons can be learned from polymer rheology; however, it should be noted that the stresses, normal, and shear, are much greater in elastohydrodynamic lubrication (EHL) than are studied in polymer rheology and rheological effects are occurring in simple liquids that are never considered to be of interest to polymer rheologists.

2.2 THE NEWTONIAN MODEL

The constitutive equation for a compressible Newtonian liquid [3] with Newtonian shear viscosity, μ, is

$$\begin{bmatrix}\sigma_{xx}\,\sigma_{xy}\,\sigma_{xz}\\ \sigma_{yx}\,\sigma_{yy}\,\sigma_{yz}\\ \sigma_{zx}\,\sigma_{zy}\,\sigma_{zz}\end{bmatrix}=$$
$$\begin{bmatrix}\mu\left(\frac{\partial u}{\partial x}+\frac{\partial u}{\partial x}\right)+\upsilon\left(\frac{\partial u}{\partial x}+\frac{\partial v}{\partial y}+\frac{\partial w}{\partial z}\right)-p & \mu\left(\frac{\partial u}{\partial y}+\frac{\partial v}{\partial x}\right) & \mu\left(\frac{\partial u}{\partial z}+\frac{\partial w}{\partial x}\right)\\ \mu\left(\frac{\partial v}{\partial x}+\frac{\partial u}{\partial y}\right) & \mu\left(\frac{\partial v}{\partial y}+\frac{\partial v}{\partial y}\right)+\upsilon\left(\frac{\partial u}{\partial x}+\frac{\partial v}{\partial y}+\frac{\partial w}{\partial z}\right)-p & \mu\left(\frac{\partial v}{\partial z}+\frac{\partial w}{\partial y}\right)\\ \mu\left(\frac{\partial w}{\partial x}+\frac{\partial u}{\partial z}\right) & \mu\left(\frac{\partial w}{\partial y}+\frac{\partial v}{\partial z}\right) & \mu\left(\frac{\partial w}{\partial z}+\frac{\partial w}{\partial z}\right)+\upsilon\left(\frac{\partial u}{\partial x}+\frac{\partial v}{\partial y}+\frac{\partial w}{\partial z}\right)-p\end{bmatrix} \tag{2.1}$$

where σ_{xx} is the normal stress component in the x-direction and σ_{xy} is the (shear) stress component in the x,y-directions of the stress tensor, $\boldsymbol{\sigma}$ (Fig. 2.1). For the normal stresses, tension is positive, leading to the minus sign on pressure. The dilation rate is $\partial u/\partial x + \partial v/\partial y + \partial w/\partial z$ and υ is a dilatational or bulk viscosity that together with μ results in a relaxation of the volume following an instantaneous change in the mechanical pressure, defined as $p_m = -\left(\sigma_{xx} + \sigma_{yy} + \sigma_{zz}\right)/3$ [4]. Such volume relaxation can be experimentally observed at pressures near to the glass transition (Chapter 4: Compressibility and the Equation of State and Chapter 9: The Glass Transition and Related Transitions in Liquids Under Pressure). For compressible flow, a distinction must be made between p_m and the thermodynamic pressure, p, that is related to the density (or volume) and the temperature through an equation of state (Chapter 4: Compressibility and the Equation of State). For compressible flow, p and p_m are related by

$$p_m = p - \left(\upsilon + \frac{2}{3}\mu\right)\left(\frac{\partial u}{\partial x} + \frac{\partial v}{\partial y} + \frac{\partial w}{\partial z}\right) \tag{2.2}$$

For an incompressible Newtonian liquid, $\partial u/\partial x + \partial v/\partial y + \partial w/\partial z = 0$, there is no distinction between p and p_m and the constitutive equation is then

$$\begin{bmatrix}\sigma_{xx} & \sigma_{xy} & \sigma_{xz}\\ \sigma_{yx} & \sigma_{yy} & \sigma_{yz}\\ \sigma_{zx} & \sigma_{zy} & \sigma_{zz}\end{bmatrix}=\begin{bmatrix}\mu\left(\frac{\partial u}{\partial x}+\frac{\partial u}{\partial x}\right)-p & \mu\left(\frac{\partial u}{\partial y}+\frac{\partial v}{\partial x}\right) & \mu\left(\frac{\partial u}{\partial z}+\frac{\partial w}{\partial x}\right)\\ \mu\left(\frac{\partial v}{\partial x}+\frac{\partial u}{\partial y}\right) & \mu\left(\frac{\partial v}{\partial y}+\frac{\partial v}{\partial y}\right)-p & \mu\left(\frac{\partial v}{\partial z}+\frac{\partial w}{\partial y}\right)\\ \mu\left(\frac{\partial w}{\partial x}+\frac{\partial u}{\partial z}\right) & \mu\left(\frac{\partial w}{\partial y}+\frac{\partial v}{\partial z}\right) & \mu\left(\frac{\partial w}{\partial z}+\frac{\partial w}{\partial z}\right)-p\end{bmatrix} \tag{2.3}$$

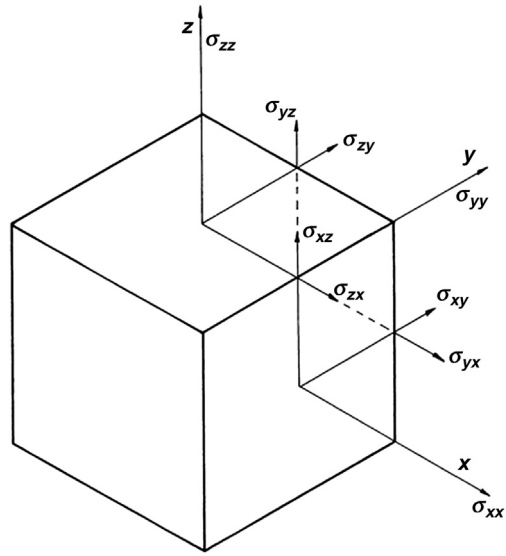

Figure 2.1 Stresses defined.

The quantities in parentheses on the right-hand side of Eq. (2.3) are the components of the rate of deformation tensor, **D**, multiplied by 2. Eq. (2.3) can be written in tensor "shorthand" as

$$\boldsymbol{\sigma} = 2\mu\,\mathbf{D} - \mathbf{I}\,p \tag{2.3a}$$

There are two simple ideal flows that are utilized for rheological experiments, simple uniaxial extension and simple shear. For simple uniaxial extension in the x-direction, the elongation strain rate is $\dot{\varepsilon} = \partial u/\partial x$, if the flow is incompressible, $\partial v/\partial y = \partial w/\partial z = -\dot{\varepsilon}/2$, and all other velocity gradients are zero. That is, for a cylindrical element of incompressible liquid being stretched at a particular elongation rate, the diameter will contract at half that rate. The off-diagonal (shear) stresses are zero and $\sigma_{yy} = \sigma_{zz}$. We shall ignore the body forces and acceleration and the only important stresses are the normal stress differences, $\sigma_{xx} - \sigma_{yy}$ or $\sigma_{xx} - \sigma_{zz}$. If we define the *elongational viscosity* as $\eta_e = \left(\sigma_{xx} - \sigma_{yy}\right)/\dot{\varepsilon}$, Eq. (2.3) gives for a Newtonian liquid,

$$\eta_e = 3\mu \tag{2.4}$$

For simple shear in the x-direction, $\partial u/\partial z = \dot{\gamma}$, the *shear rate*, and the other velocity gradients are zero. Eq. (2.1) or (2.3) yields for a Newtonian liquid,

$$\sigma_{xz} = \sigma_{zx} = \tau = \mu\dot{\gamma} \tag{2.5}$$

as it should. The other shear stresses are zero and the first and second normal stress differences are

$$N_1 = \sigma_{xx} - \sigma_{zz} = 0 \quad \text{and} \quad N_2 = \sigma_{zz} - \sigma_{yy} = 0 \tag{2.6}$$

Simple shear has a special importance for rheological experiments related to lubrication.

Experimental measurements for polymeric liquids can yield very different results from the predictions of the Newtonian model. All of the data presented in this chapter should be understood to have been obtained at ambient pressure.

2.3 MATERIAL FUNCTIONS FOR POLYMERIC LIQUIDS

2.3.1 Shear viscosity

For polymeric liquids, the shear viscosity is a function of shear rate (or stress) and a generalized or non-Newtonian viscosity is defined in simple shear as $\eta(\dot{\gamma}) = \tau/\dot{\gamma}$ or $\eta(\tau) = \tau/\dot{\gamma}$. This is illustrated in Fig. 2.2 where the logarithm of the steady shear viscosity at 150°C of a molten low-density polyethylene is plotted against the logarithm of shear rate. This information is presented in the form of a graph called a *flow curve*. The

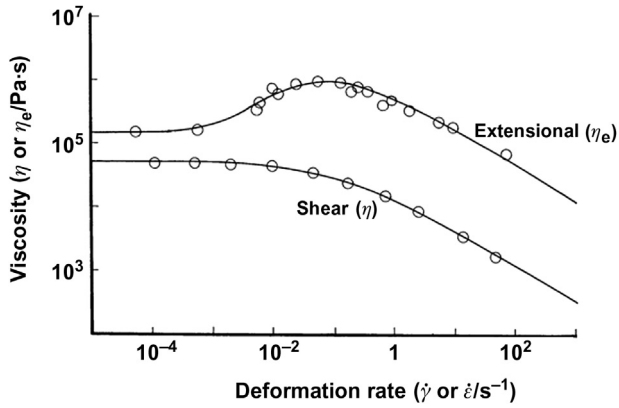

Figure 2.2 The steady shear viscosity and steady elongational viscosity of a polyethylene melt from [5]. *Reprinted with permission from Elsevier.*

steady elongational viscosity is also plotted against elongation rate. The shear viscosity is seen to monotonically decrease with shear rate in Fig. 2.2, a phenomenon known as *shear-thinning*. This effect is clearly most import for lubrication as the property of viscosity provides the load-supporting pressure that is described by the Reynolds equation (1.17). If the Newtonian viscosity, μ, is replaced by the shear-dependent viscosity, η, in the incompressible Newtonian constitutive Eq. (2.3), the result is the incompressible *generalized Newtonian fluid* model,

$$\boldsymbol{\sigma} = 2\eta\,\mathbf{D} - \mathbf{I}\,p \tag{2.7}$$

Of course for flows more complicated than simple shear, the argument of the viscosity function requires some consideration. The viscosity must depend upon a quantity that is independent of the way the coordinate system is specified. Then it should depend on some combination of the three scalar invariants of either the strain rate tensor, $\mathbf{D}$, or of the deviatoric stress tensor, $\boldsymbol{\sigma} + \mathbf{I}\,p$ [1]. The deviatoric stress is used in place of the total stress so that a hydrostatic pressure can not affect flow other than through its effect on the low shear viscosity. If we define the magnitude of the strain rate tensor, $\dot{\gamma}^*$, so that it will be the argument for the viscosity function, one of the invariants is zero for shear flows and another is zero for incompressible flow [1], leaving the second invariant as the choice for an argument of the function, $\eta(\dot{\gamma}^*)$. There are a number of different ways to write the second invariant and for the purpose of replacing $\dot{\gamma} = \partial u/\partial z$ as the definition of $\dot{\gamma}^*$, the following relation is consistent with simple shear measurements where $\dot{\gamma}^* = \partial u/\partial z$.

$$\dot{\gamma}^* = \sqrt{\left(\frac{\partial u}{\partial y} + \frac{\partial v}{\partial x}\right)^2 + \left(\frac{\partial u}{\partial z} + \frac{\partial w}{\partial x}\right)^2 + \left(\frac{\partial w}{\partial y} + \frac{\partial v}{\partial z}\right)^2 + 2\left(\frac{\partial u}{\partial x}\right)^2 + 2\left(\frac{\partial v}{\partial y}\right)^2 + 2\left(\frac{\partial w}{\partial z}\right)^2} \tag{2.8}$$

Following a similar argument, if viscosity is to depend upon stress as $\eta(\tau^*)$, the appropriate invariant of the deviatoric stress tensor is [1]

$$\tau^* = \sqrt{\frac{(\sigma_{xx}+p)^2}{2} + \frac{(\sigma_{yy}+p)^2}{2} + \frac{(\sigma_{zz}+p)^2}{2} + (\sigma_{xy})^2 + (\sigma_{xz})^2 + (\sigma_{yz})^2} \tag{2.9}$$

where $\tau^* = \sigma_{xz} = \sigma_{zx}$ in simple shear. For a purely hydrostatic state of stress, $\sigma_{xx} = \sigma_{yy} = \sigma_{zz} = -p$, and $\tau^* = 0$ as expected. These relationships are useful for the incompressible generalized Newtonian fluid.

Examples of expressions for the viscosity function used in the generalized Newtonian fluid model are the Cross equation [6],

$$\eta(\dot{\gamma}^*) = \mu_2 + \frac{\mu - \mu_2}{1 + \left|\lambda\dot{\gamma}^*\right|^{1-n}} \tag{2.10}$$

and the Ellis equation [7],

$$\eta(\tau^*) = \mu_2 + \frac{\mu - \mu_2}{1 + \left|\tau^*/\tau_c\right|^{((1/n)-1)}} \tag{2.11}$$

Here, n, is the power-law exponent, λ is a characteristic time, and τ_c is a characteristic stress. The dimensionless $Wi = \lambda\dot{\gamma}^*$ is the Weissenberg number for the flow. For the liquid in Fig. 2.2, at shear rate less than $10^{-3}\ \mathrm{s}^{-1}$, the viscosity is reasonably constant and approaches a limiting value we call the *limiting low shear viscosity*, μ, and the low shear regime for which $\eta \approx \mu$ is the *terminal regime*. In the rheology literature, the low shear viscosity is typically given the term η_0, instead of μ, to differentiate the terminal behavior of a shear-thinning liquid from constant viscosity of a Newtonian liquid. In the elastohydrodynamic literature, the subscript, "$_0$" is typically reserved for the value of a property at ambient pressure. Therefore, the same variable name, μ, is used here for both the Newtonian viscosity and the low shear viscosity to avoid confusion when considering the pressure dependence of viscosity. The second Newtonian viscosity, μ_2, may appear in measurements as a limiting high shear viscosity, although no limiting high shear Newtonian behavior can be observed in Fig. 2.2.

The generalized Newtonian model is extremely useful in engineering calculations of flow but it has some interesting limitations to be seen in the next sections.

2.3.2 Elongational viscosity

The steady elongational viscosity, $\eta_e = \left(\sigma_{xx} - \sigma_{yy}\right)/\dot{\varepsilon}$, is plotted in Fig. 2.2 for the polyethylene melt. In the terminal regime $\eta_e \approx 3\eta$, as the Newtonian model predicts but this relationship does not hold for higher deformation rates. The elongational viscosity first increases with elongation rate, and then decreases. The shear viscosity function when implemented in the generalized Newtonian model is not helpful for extensional viscosity. Extensional viscosity is important in tribology for squeeze film lubrication.

There is another complication as well. If the direction of a simple shear is reversed, the same value of shear viscosity will be observed. The absolute value function appears in Eqs. (2.9) and (2.10). Reversing the direction of elongation will not generally yield the same elongational viscosity.

For elastohydrodynamics, the elongation component of the flow should be insignificant compared with shear flow. Tanner [3] has investigated the effect of elongation on a simple squeeze film lubrication flow and found that the elongational contribution to the load was insignificant for the usual EHL thin films. We will not consider elongation further.

2.3.3 Normal stress differences

Shear-thinning is generally accompanied by the rapid development of differences in the normal stresses in simple shear. This nonintuitive effect is similar to the behavior of rubbery elastic solids that are subjected to a simple shear strain that is greater than the infinitesimal assumption. For rubber at large shear strain, the shear stress is linear with strain but the difference between the tension in the flow direction and the tension in the cross-flow direction increases with the square of the shear strain [8]. If unconstrained, the separation between the parallel shearing faces of a block of the solid will grow.

Normal stress differences for steady shear of a polymer solution of polyisobutylene in decalin, a low molecular weight cyclic hydrocarbon, are illustrated in the flow curves in Fig. 2.3. In this case, the flow curves are in the form of the logarithm of stress plotted against the logarithm of shear rate. The shear stress, τ, can be seen to follow a power-law function of the shear rate,

$$\tau \propto \dot{\gamma}^n \tag{2.12}$$

usually known as the Ostwald-de Waele equation with $n = 0.53$. A weakness of this model is the lack of terminal behavior. The normal stress differences, $N_1 = \sigma_{xx} - \sigma_{zz}$ and $N_2 = \sigma_{zz} - \sigma_{yy}$, also follow a power-law but with much larger power-law exponents than the shear stress. Motion is in the x-direction. Notice that $N_1 > 0$ and $N_2 < 0$ and $|N_2| \approx |N_1|/10$ for this liquid. The first normal stress difference in Fig. 2.3 is much larger than the shear stress and this behavior may be observed in polymer thickened lubricants as well [9]. The generalized Newtonian fluid model (2.7) does not predict these stress differences.

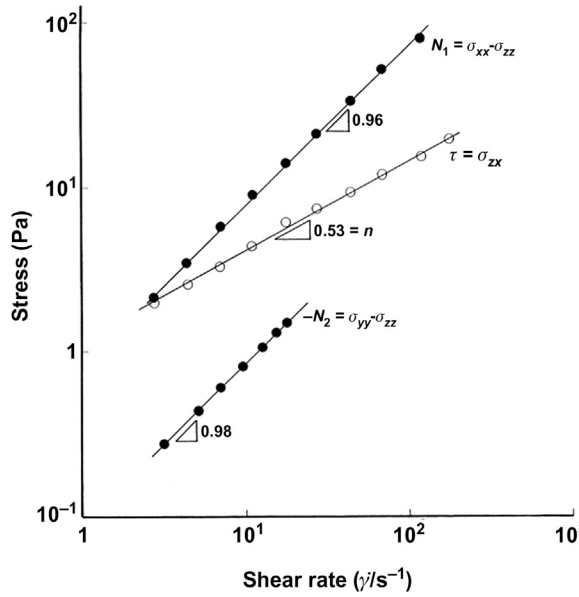

Figure 2.3 The shear rate dependence of shear stress, τ, first normal stress difference, N_1, and second normal stress difference, N_2, for a 1.1% polyisobutylene in decalin solution from [10]. *Reprinted with permission from Elsevier.*

The measurement of N_1 has become relatively routine, while N_2 requires difficult specialized laboratory technique. For Fig. 2.3, the shear stress and N_1 were obtained from the torsional flow between a rotating cone and a coaxial stationary circular disc. The torque to restrain the rotation of the stationary disc yields the shear stress and the normal force required to prevent the separation of the cone and plate yields N_1. A pressure profile is generated by N_1 that supports a normal load. Notice that the Newtonian based Reynolds equation (1.11) of Chapter 1, An Introduction to Elastohydrodynamic Lubrication, does not predict a pressure profile for this geometry. There is no change in film thickness in the flow direction, $dh/dx = 0$ in Eq. (1.11). Then the pressure gradient in the flow direction must be constant from (1.11) and must be zero for the pressure to be continuous around the gap.

The measurement of N_2 in Fig. 2.3 was provided by analysis of the shape of the free surface of liquid flowing downhill in an open channel. See Ref. [10] for a complete description of the technique. Until about 60 years ago, it was supposed that N_2 was zero and this assumption is known as the Weissenberg hypothesis.

When the direction of shear, $\partial u/\partial z = \dot{\gamma}$, is reversed in a simple shear experiment, the direction of the shear stress, $\sigma_{zx} = \tau$, changes; however, symmetry requires that the normal stress differences $\sigma_{xx} - \sigma_{zz} = N_1$ and $\sigma_{zz} - \sigma_{yy} = N_2$ be independent of the direction of shear. That is, the normal stress differences must be even functions of $\dot{\gamma}$ while shear stress is an odd function. This requirement suggests that the definitions of the normal stress coefficients, ψ_1 and ψ_2, should be given by $N_1 = \psi_1\dot{\gamma}^2$ and $N_2 = \psi_2\dot{\gamma}^2$. It is usually found that in the terminal regime, N_1 varies with $\dot{\gamma}^2$ or τ^2, in other words, that like viscosity, ψ_1 is constant.

Some methods of calculating N_1 from the way that the viscosity varies with shear have been advanced, see Ref. [11] for examples. These methods should be limited to special cases because of the discovery of liquids which generate a large first normal stress difference while the viscosity appears to be independent of shear [12]. These *Boger liquids* are dilute solutions of high molecular weight polymer in a low molecular weight, but vary viscous, solvent such as polybutene. Then the polymer contribution to the viscosity is small.

2.4 RHEOLOGICAL MODELS

2.4.1 Viscoelastic models

The experiments and models described to this point have considered steady-state deformation rates. If the shear rate in a polymeric liquid is imposed quickly enough, the stress may require some time to reach the steady value and may even overshoot the steady value if the strain rate is high. If the strain rate is applied periodically as a sinusoidally varying function of time, a component of stress will appear that is out of phase with the strain rate. These phenomena, like the normal stress differences, cannot be predicted by the generalized Newtonian model.

In classical elasticity, the stress depends on strain and not on strain rate. In Newtonian fluid mechanics, the stress depends on strain rate and not on the strain. The behavior described above indicates that polymeric liquids can have the attributes of both viscosity and elasticity simultaneously. Models that combine an elastic modulus and a viscosity are time-dependent. The first and perhaps the most simple viscoelastic model is the

single mode Maxwell model that sums a strain rate due to elasticity, $\partial(\tau/G)/\partial t$, with a strain rate due to viscous flow, τ/μ, to obtain for constant shear modulus, G,

$$(\boldsymbol{\sigma} + \mathbf{I}p) + \frac{\mu}{G}\frac{\partial}{\partial t}(\boldsymbol{\sigma} + \mathbf{I}p) = 2\mu\mathbf{D} \tag{2.13}$$

The time derivative of the deviatoric stress in the equation above requires special care when the strains are not infinitesimal. It must be formulated to be independent of the chosen reference frame. There are three main objective time derivatives, the corotational (or Jaumann) derivative and the upper and lower convected derivatives, that may be substituted for $\partial/\partial t$ in Eq. (1.13). Joseph [13] has defined an interpolated invariant derivative that provides for a continuous mix of the three.

The Jaumann derivative has been employed extensively in lubrication, see Ref. [14], for example, and when used in the Maxwell model (2.13), yields some aspects of measurable steady shear response. The material derivative is

$$\frac{D}{Dt} = \frac{\partial}{\partial t} + u\frac{\partial}{\partial x} + v\frac{\partial}{\partial y} + w\frac{\partial}{\partial z} \tag{2.14}$$

The x,y element of the vorticity tensor is

$$\omega_{xy} = -\omega_{yx} = \frac{1}{2}\left(\frac{\partial v}{\partial x} - \frac{\partial u}{\partial y}\right) \tag{2.15}$$

and so on. Then the Jaumann derivative for the x,z component, σ_{xz}, of the stress tensor is, for an example,

$$\frac{\mathbf{D}\sigma_{xz}}{\mathbf{D}t} = \frac{D\sigma_{xz}}{Dt} + \left\{\omega_{xx}\sigma_{xz} + \omega_{xy}\sigma_{yz} + \omega_{xz}\sigma_{zz} - \sigma_{xx}\omega_{xz} - \sigma_{xy}\omega_{yz} - \sigma_{xz}\omega_{zz}\right\} \tag{2.16}$$

The derivatives of the other components follow the same rule.

For the steady simple shear experiment that has been employed as a previous example, $\partial u/\partial z = \dot{\gamma}$, and the other velocity gradients are zero. The stress gradients are zero and the stresses are steady. Then the material derivatives of the stress components with respect to time are zero. Solving then

$$(\boldsymbol{\sigma} + \mathbf{I}p) + \frac{\mu}{G}\frac{\mathbf{D}}{\mathbf{D}t}(\boldsymbol{\sigma} + \mathbf{I}p) = 2\mu\mathbf{D} \tag{2.17}$$

for $\sigma_{xz} = \sigma_{zx} = \tau$ yields,

$$\sigma_{xz} + \frac{\mu}{G}\left\{\frac{\partial \sigma_{xz}}{\partial t} + u\frac{\partial \sigma_{xz}}{\partial x} + v\frac{\partial \sigma_{xz}}{\partial y} + w\frac{\partial \sigma_{xz}}{\partial z} + \frac{1}{2}\left[\sigma_{yz}\left(\frac{\partial v}{\partial x} - \frac{\partial u}{\partial y}\right) + \sigma_{xy}\left(\frac{\partial v}{\partial z} - \frac{\partial w}{\partial y}\right) + \left(\sigma_{zz} - \sigma_{xx}\right)\left(\frac{\partial w}{\partial x} - \frac{\partial u}{\partial z}\right)\right]\right\} = \mu\left(\frac{\partial u}{\partial z} + \frac{\partial w}{\partial x}\right) \tag{2.18}$$

The above simplifies to

$$\tau + \frac{\mu\dot{\gamma}}{2G}(\sigma_{xx} - \sigma_{zz}) = \mu\dot{\gamma} \tag{2.19}$$

Similarly solving (2.17) for σ_{xx}, σ_{zz}, and σ_{yy},

$$\sigma_{xx} + p = \frac{\mu\dot{\gamma}}{G}\tau, \quad \sigma_{zz} + p = -\frac{\mu\dot{\gamma}}{G}\tau, \quad \text{and} \quad \sigma_{yy} + p = 0 \tag{2.20}$$

Combining (2.19) and (2.20) gives,

$$\tau = \frac{\mu\dot{\gamma}}{1 + \left(\mu\dot{\gamma}/G\right)^2} \quad \text{and} \quad \eta = \frac{\mu}{1 + \left(\mu\dot{\gamma}/G\right)^2} \tag{2.21}$$

$$N_1 = \sigma_{xx} - \sigma_{zz} = \frac{2G\left(\mu\dot{\gamma}/G\right)^2}{1 + \left(\mu\dot{\gamma}/G\right)^2} \tag{2.22}$$

$$N_2 = \sigma_{zz} - \sigma_{yy} = -\frac{N_1}{2} \tag{2.23}$$

The elongational viscosity for the corotational Maxwell model is $\eta_e = 3\mu$.

These results may be compared to the data for a non-Newtonian standard reference material [15] in Fig. 2.4. The National Institute for Science and Technology (NIST) has thoroughly characterized the steady shear and dynamic shear properties of two polymeric liquids. The shear stress and the first normal stress difference are plotted in Fig. 2.4 for the dimethyl silicone SRM 2491 in steady shear at two temperatures as shown in the figure. The data in Fig. 2.4 do not penetrate far into the nonlinear regime and using a value of $G = 9000$ Pa in Eqs. (2.21) and (2.22) results in the curves plotted in the figure. First, the corotational Maxwell model represents the available shear stress data well, but at higher shear rates the shear stress displays a local maximum and then decreases with increasing

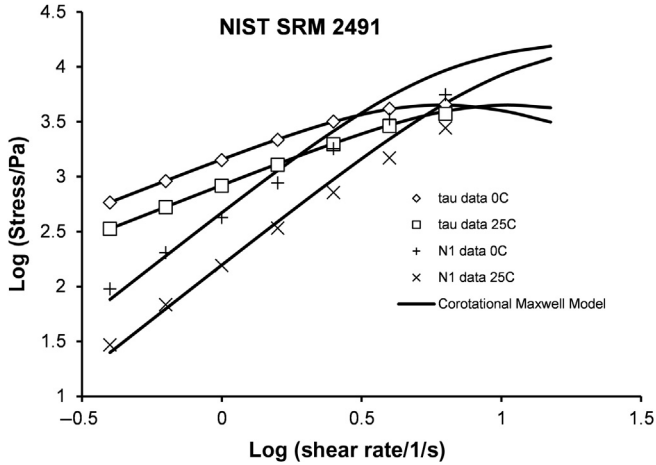

Figure 2.4 The shear rate dependence of shear stress, τ, and first normal stress difference, N_1, at two temperatures, 0°C and 25°C, for a non-Newtonian standard reference material, a dimethyl siloxane. The corotational Maxwell model with $G = 9$ kPa is shown as the curves. *Data from Schultheisz CR, Flynn KM, Leigh SD. Certification of the rheological behavior of SRM 2491, polydimethylsiloxane. NIST Special Publication 260-147; 2001.*

rate as can be seen in Fig. 2.4. This response is not generally acceptable as nonmonotonic flow curves can result in a constitutive instability and banded shear flows where two shear rates can coexist in the same flow. Comparing, however, the N_1 data with the corotational Maxwell model shows good agreement in the terminal regime but not at higher shear rates. Then the corotational Maxwell model predicts shear-thinning that is overly severe but the prediction for the first normal stress difference is reasonable at low shear rates. The magnitude of the second normal stress difference, Eq. (2.23), is in general too large, but the sense is correct. The second normal stress difference is not shown in Fig. 2.4.

There is another interesting property of the single mode Maxwell model. For small strain oscillatory simple shear with $\gamma = \gamma_A \sin \omega t$ and $\dot{\gamma} = \gamma_A \omega \cos \omega t$, the time derivative in Eq. (2.13) is appropriate and we have,

$$\frac{d\tau}{dt} + \frac{G}{\mu}\tau = G\gamma_A \omega \cos \omega t \tag{2.24}$$

where γ_A is the shear strain amplitude and ω is the angular frequency. This linear first-order equation has the solution

$$\tau = \frac{(\mu^2 \omega \gamma_A / G)}{1 + (\mu\omega/G)^2} \left[\frac{G}{\mu} \cos \omega t + \omega \sin \omega t \right] \tag{2.25}$$

where the shear stress in phase with the shear rate and the dynamic viscosity are,

$$\tau' = \frac{\mu \gamma_A \omega \cos \omega t}{1 + (\mu\omega/G)^2} \quad \text{and} \quad \eta' = \tau'\dot{\gamma} = \frac{\mu}{1 + (\mu\omega/G)^2} \tag{2.26}$$

Compare this result for the dynamic viscosity, $\eta'(\omega)$, with the steady shear result for $\eta(\dot{\gamma})$ in Eq. (2.21). They are equivalent expressions. This *analogy between continuous and oscillatory shear* has been used extensively in elastohydrodynamics although, experimentally, it sometimes fails to be accurate at large shear rates far beyond the terminal regime. Dyson [16] had some success in applying this analogy to the rheology of silicone oils and predicting the film thickness in line contact using viscosity measured at high frequency. There is experimental advantage to be gained through the use of small strains and high frequencies as a substitute for high shear rates. The viscous heating, which substantially limits the shear rates that can be attained isothermally, is rarely a problem in dynamic measurements. This technique was unfortunately abandoned by elastohydrodynamics about 30 years ago. An excellent exposition on the dynamic properties of liquids that includes high-pressure effects can be found in Harrison [17].

Other objective time derivatives can be utilized for the Maxwell model. The upper convected derivative results in the shear viscosity being constant and the elongational viscosity being unbounded at some strain rates. Also $N_1 = 2\mu^2\dot{\gamma}^2/G$ and $N_2 = 0$. There are other ways of combining elastic and viscous components in addition to the Maxwell approach.

It may be useful to substitute one of the shear-thinning viscosity functions, $\eta(\dot{\gamma}^*)$, into the Maxwell model (2.13) for infinitesimal strain. If a convected time derivative is employed, the White–Metzner model will be the result [1]. Viscosity functions for this purpose can be found in the next section.

2.4.2 Generalized Newtonian fluid models

The generalized Newtonian model can be useful for engineering calculations of flow, although we have seen that it lacks sufficient detail to

describe many non-Newtonian effects. Since the Reynolds equation is essentially a flow conservation equation, the usefulness of the generalized Newtonian model for lubrication problems should be apparent. The two viscosity functions introduced in Eqs. (2.10) and (2.11) require parameters, λ and τ_c, respectively, that characterize the limit of the terminal (constant viscosity) regime.

The relative viscosity and first normal stress difference of another NIST non-Newtonian standard reference liquid, SRM 2490, a polymer solution, is shown in Fig. 2.5 plotted against shear stress. The relative viscosity, η/μ, data for three temperatures are shown as superimposing to form a master curve at the top graph of Fig. 2.5. Plotting η/μ against shear rate does not superimpose the data in this way. The normal stress data for three temperatures are shown as superimposing to form a master curve at the bottom graph of Fig. 2.5. This ability to normalize data by presenting properties as functions of shear stress (or as a function of $\mu\dot{\gamma}$) is a general feature of shear-thinning. The Cross equation (2.10) is plotted as the curve in the top of Fig. 2.5 using parameters supplied by NIST [18], $n = 0.18$ and $\mu_2 = 0$.

$$\eta(\dot{\gamma}) = \mu_2 + \frac{\mu - \mu_2}{1 + \left|\lambda\dot{\gamma}\right|^{1-n}} \tag{2.10}$$

Here, the characteristic time, λ, has been written as a Maxwell relaxation time,

$$\lambda = \frac{\mu}{G} \tag{2.27}$$

with $G = 428$ Pa. The approximation of the characteristic time with a viscoelastic relaxation time can be justified. Bird et al. [1] state "...experimental data, many molecular theories, and many nonlinear viscoelastic constitutive equations do show a connection between the time constant determined from ... the $\eta(\dot{\gamma})$ expression ... and that determined from ...linear viscoelasticity...." The Cross equation with $G = 428$ Pa is an excellent fit to the viscosity data in Fig. 2.5 for all three temperatures. The corotational Maxwell model gives for the terminal regime (see Eq. (2.22) for $\mu\dot{\gamma} \ll G$),

$$N_1 \approx \frac{2\tau^2}{G} \tag{2.28}$$

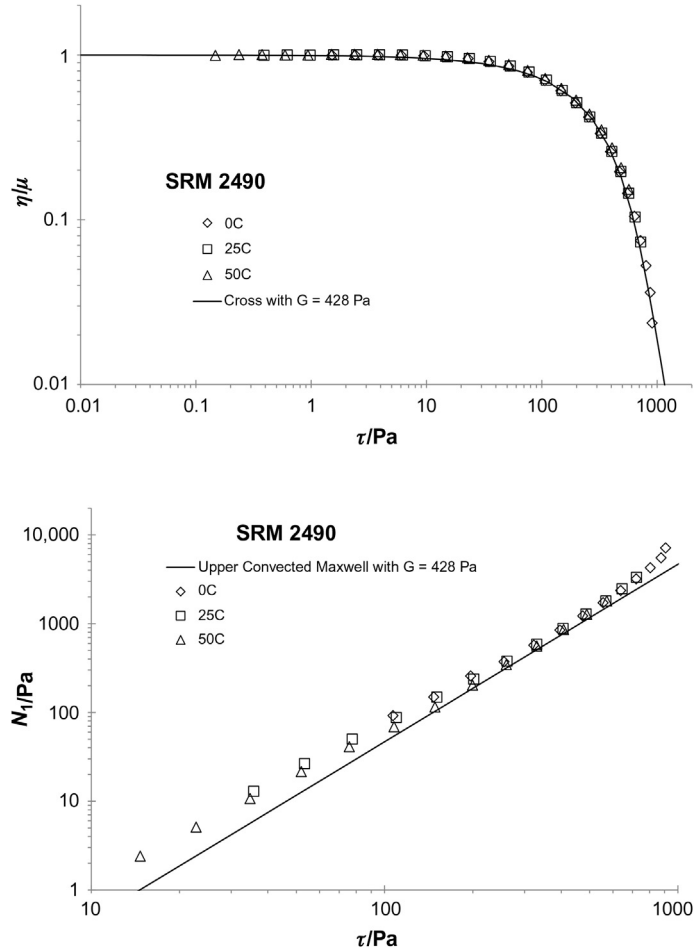

Figure 2.5 The shear stress dependence of the relative viscosity, η/μ, top, and the first normal stress difference, N_1, bottom, for a non-Newtonian standard reference material, a solution of polyisobutylene in pristane, from [18] at three temperatures, 0°C, 25°C, and 50°C.

and the upper convected Maxwell model predicts this relationship for all shear stress. This relationship is plotted in the bottom graph of Fig. 2.5 and shows good agreement with the data. If we substitute $G = \tau_c$ in the $\eta(\tau)$ expressions, then it will be shown in the following that we have a consistent way to write all of the ordinary viscosity functions.

The Cross equation (2.10) and the Ellis equation with G replacing τ_c,

$$\eta(\tau) = \mu_2 + \frac{\mu - \mu_2}{1 + \left|\tau/G\right|^{((1/n)-1)}} \tag{2.29}$$

are plotted in Fig. 2.6 with $\mu = 10$, $\mu_2 = 10^{-3}$, $\lambda = 1$, $G = \mu/\lambda = 10$, and $n = 0.4$ using arbitrary units. The two viscosity functions are approximately the same in the terminal regime, $\tau = \mu\dot{\gamma}$, and power-law regime, $\tau = G(\lambda\dot{\gamma})^n$, where thin straight lines represent these relationships in Fig. 2.6. The lines intersect at $\lambda\dot{\gamma} = 1$ and $\tau/G = 1$. That is, $\lambda\dot{\gamma} = 1$ and $\tau/G = 1$ establish the approximate limit of Newtonian response by specifying the rate, $\dot{\gamma}$, or stress, τ, respectively, at the intersection of lines tangent to the terminal regime and to the power-law regime. All of the ordinary viscosity functions explicitly incorporating the power-law exponent, n, share this property provided that μ_2 is small compared with μ or is zero. When μ/μ_2 is not very much larger than one, then the power-law regime never fully develops.

Table 2.1 lists the viscosity functions already mentioned and, in addition, the Spriggs truncated power-law [19], Ferry [20], Rabinowitsch

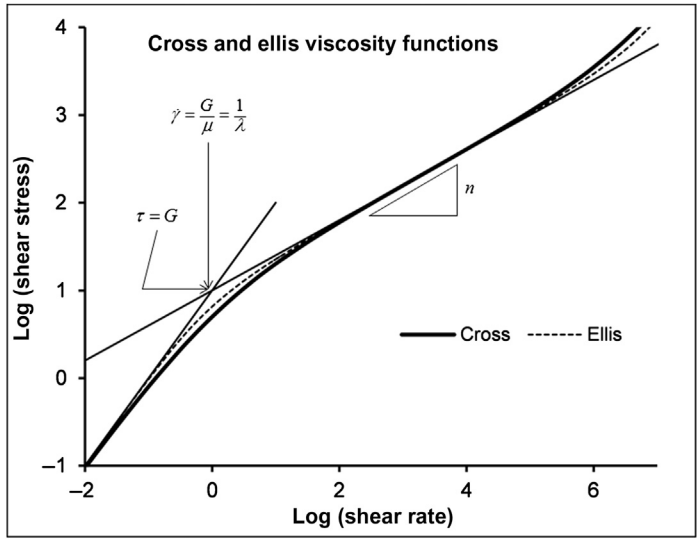

Figure 2.6 The shear stress, τ, versus shear rate, $\dot{\gamma}$, for two viscosity functions using $\mu = 10$, $\mu_2 = 10^{-3}$, $\lambda = 1$, $G = \mu/\lambda = 1$, and $n = 0.4$ with arbitrary units. The fine lines represent the terminal regime, $\tau = \mu\dot{\gamma}$, and the power-law regime, $\tau = G(\lambda\dot{\gamma})^n$, that are approximately tangent to the viscosity functions. The intersection occurs at $\tau = G$ and $\dot{\gamma} = 1/\lambda$.

Table 2.1 Viscosity functions for the generalized Newtonian fluid model

$\eta(\dot{\gamma})$		$\eta(\tau)$	
$\eta = \mu$	Newtonian	$\eta = \mu$	Newtonian
$\eta = \mu\lvert\lambda\dot{\gamma}\rvert^{n-1}$	Ostwald-de Waele	$\eta = \mu\lvert\frac{\tau}{G}\rvert^{1-(1/n)}$	Ostwald-de Waele
$\eta = \begin{matrix}\mu, \lvert\lambda\dot{\gamma}\rvert \le 1 \\ \mu\lvert\lambda\dot{\gamma}\rvert^{n-1}, \lvert\lambda\dot{\gamma}\rvert \ge 1\end{matrix}$	Spriggs [19]	$\eta = \begin{matrix}\mu, \lvert\tau/G\rvert \le 1 \\ \mu\lvert\tau/G\rvert^{1-(1/n)}, \lvert\tau/G\rvert \ge 1\end{matrix}$	Spriggs [19]
$\eta = \mu_2 + \frac{\mu-\mu_2}{1+\lvert\lambda\dot{\gamma}\rvert^{1-n}}$	Cross [6]	$\eta = \mu_2 + \frac{\mu-\mu_2}{1+\lvert\tau/G\rvert^{((1/n)-1)}}$	Ellis [7]
		$\eta = \mu_2 + \frac{\mu-\mu_2}{1+\lvert\tau/G\rvert}$	Ferry [20]
		$\eta = \mu_2 + \frac{\mu-\mu_2}{1+(\tau/G)^2}$	Rabinowitsch [21]
$\eta = \mu_2 + \frac{\mu-\mu_2}{\left[1+(\lambda\dot{\gamma})^2\right]^{(1-n)/2}}$	Carreau [22]	$\eta = \mu_2 + \frac{\mu-\mu_2}{\left[1+\left(\frac{\tau}{G}\right)^2\right]^{((1/n)-1)/2}}$	Bair and Khonsari [23]
$\eta = \mu_2 + \frac{\mu-\mu_2}{\left[1+(\lambda\dot{\gamma})^a\right]^{(1-n)/a}}$	Carreau-Yasuda [23]	$\eta = \mu_2 + \frac{\mu-\mu_2}{\left[1+\lvert\tau/G\rvert^a\right]^{((1/n)-1)/a}}$	Bair [25]
$\eta = \sum_{i=1}^{N} \frac{f_i\mu}{\lambda_i\dot{\gamma}} \sinh^{-1}(\lambda_i\dot{\gamma})$	Ree–Eyring [25]		
$\sum_{i=1}^{N} f_i = 1, \quad N > 1$			

[21], Carreau [22], Carreau-Yasuda [3], two models introduced by the author's laboratory [23,24], and the Ree–Eyring [25] model. The Ree–Eyring equation differs from the other ordinary viscosity functions in that it does not explicitly incorporate the power-law exponent, n. In the way that Eyring made use of this relation [25], it is clear that he intended it to be used to describe terminal, power-law, and possibly second Newtonian behavior.

2.5 TIME–TEMPERATURE–PRESSURE SUPERPOSITION

When flow curves obtained at different temperatures (or pressures) for one material are plotted as $\log\eta$ versus $\log\dot{\gamma}$, the curves have the same shape. The relationships between the variables have the same functional form. The same holds true for $\log\tau$ versus $\log\dot{\gamma}$ or $\log\eta$ versus $\log\tau$. We have already seen in Fig. 2.5 that relative viscosity, η/μ, or the first normal stress difference measured for different temperatures can be reduced to essentially a single flow curve when the data are presented as a function of shear stress. This is a simple form of the tremendously useful principle known as *time–temperature–pressure superposition* or the *method of reduced variables*. More often "pressure" is omitted from the first name since most measurements do not include pressure as a variable. For the ordinary viscosity functions given in Table 2.1, and for the corotational Maxwell viscosity, Eq. (2.21), if n and G are held constant and only μ, and of course $\lambda = \mu/G$, vary with temperature and pressure, the simple shifting rule above will result. This concept allows the experimenter to generate rheological data under experimentally convenient conditions and obtain from that data accurate estimates of the response at conditions which may be too severe for an experimental measurement. The most obvious application is to the determination of the viscosity function at high shear rates. The high shear measurement is often a problem due to the viscous heating at high shear rate combined with the requirement that the stress be sufficiently large to penetrate into the shear-thinning regime. The alternative is to perform the measurement at low temperature (high pressure) where large shear stress can be obtained at low shear rate and with manageable heating, then shift the data to the desired temperature (pressure) and shear rate.

Tanner [3] provides a recipe for shifting of any viscosity function obtained at a reference state, T_R, p_R, that is written as $\tau = \dot{\gamma}\eta\left(\dot{\gamma}, \mu_R, \lambda_R, n_R\right)$. The shifting to another state is accomplished by replacing $\dot{\gamma}$ by $a_t\dot{\gamma}$ where a_t is the horizontal shift factor, $a_t = \left(\mu/\mu_R\right)\left(\left(\rho_R T_R\right)/(\rho T)\right)$ and τ is replaced by $F\tau$ where F is the vertical shift factor, $F = \left(\rho_R T_R\right)/(\rho T)$. The subscript "$_R$" refers to the value of the property at the reference temperature and reference pressure. The power-law exponent is not shifted, $n_R = n$. Then the shifted form is $F\tau = a_t\dot{\gamma}\eta\left(a_t\dot{\gamma}, \mu_R, \lambda_R, n\right)$. This is the standard form of time–temperature–pressure superposition sometimes called the Ferry shifting rule [26]. The shifted Cross equation (2.10) becomes

$$\frac{\rho_R T_R}{\rho T}\tau = \frac{\mu}{\mu_R}\frac{\rho_R T_R}{\rho T}\dot{\gamma}\left\{\mu_{2_R} + \frac{\left(\mu_R - \mu_{2_R}\right)}{1 + \left|\lambda_R(\mu/\mu_R)(\rho_R T_R/\rho T)\dot{\gamma}\right|^{1-n}}\right\} \tag{2.30}$$

Tanner [3] points out that compared with μ/μ_R, the quantity $\left(\rho_R T_R\right)/(\rho T)$ is close to unity for most changes of temperature (or pressure). Then if $\mu_2 = 0$, Eq. (2.30) can be approximated by

$$\eta = \tau\dot{\gamma} = \frac{\mu}{1 + \left|\lambda_R(\mu/\mu_R)\dot{\gamma}\right|^{1-n}} \tag{2.31}$$

Since $\lambda_R = \mu_R/G_R$,

$$\frac{\eta}{\mu} = \frac{1}{1 + \left|(\mu\dot{\gamma}/G_R)\right|^{1-n}} \tag{2.32}$$

Now, a plot of η/μ versus $\mu\dot{\gamma}$ will yield the same curve regardless of temperature and pressure. This simple rule has been called the Vinogradov–Malkin rule [26] and is equivalent to correlating η/μ with shear stress.

The standard shifting rule can be obtained from theory [1]. Molecular-based kinetic theory provides a theoretical foundation for the characteristic time, λ. Kinetic theory uses simple models of molecules to calculate the rheological behavior of polymers. The hydrodynamic force and the mass are concentrated at "beads" and the beads are connected by "springs" or rigid "rods". A thorough discussion of the subject can be found in Ref. [27]. For simple shearing of a solution of rigid dumbbells [27],

$$\lambda = \frac{(\mu - \mu_s)M}{c\rho R_g T} \tag{2.33}$$

where μ_s is the viscosity of the solvent (zero for neat liquid polymer), c is the concentration (one for neat liquid polymer), M is the molecular weight of the polymer, and R_g is the universal gas constant. Other models may yield a slightly different result, that is, with a leading coefficient on the right-hand side. For a neat liquid polymer, $c = 1$ and $\mu_s = 0$, and then $\lambda = \mu M/(\rho R_g T)$. Since $G = \mu/\lambda$,

$$G = \frac{\rho R_g T}{M} \tag{2.34}$$

a relationship that will be very useful later for lubricant base oils. Then the critical shear stress for the limit of Newtonian behavior varies inversely with molecular weight. Further, the ratio of characteristic times is

$$\frac{\lambda}{\lambda_R} = \frac{\mu \rho_R T_R}{\mu_R \rho T} = a_t \tag{2.35}$$

the horizontal shift factor used in temperature, pressure shifting.

Comparisons of Eq. (2.33) with tables of parameters for a viscosity function for a polymer solution, polystyrene [1], for example, show that it is only roughly correct, with an error of as great as a factor of 3 as λ varies by two orders-of-magnitude. However, the molecular weight of a liquid polymer us not as straightforward as the molecular weight of a simple liquid such as, for example, squalane, hexamethyltetracosane, for which the precise formula molecular weight is known to be 422.8 kg/kmol. The molecular weight of a polymer is specified by an average value from a distribution of molecular weight. They are polydisperse rather than monodisperse like squalane. Different parts of the molecular weight distribution may contribute differently to the viscosity, shear-thinning, and normal stress differences. The rheological techniques in the chapters that follow will provide an opportunity to evaluate expressions like (2.34) using well defined, monodisperse liquids.

There are situations in which time–temperature–pressure superposition may not superimpose flow curves from a rheological measurement. This may be the result of viscous heating so that the flow curve is not isothermal or the molecules may have been permanently degraded by the stress or it may be the result of a failure of the liquid in somewhat the same manner that a solid can be said to fail.

2.6 LIQUID FAILURE

Hutton [28] may have originated the term "liquid failure". He lists, in addition to molecular degradation, various instabilities such as edge fracture in torsional shear [8], fracture in hydrostatic tension [29], and fracture in elongational flow [8]. To these may be added, cavitation in shear flow [30], slip at the solid/liquid interface [8], slip within the liquid and banded shear flows where regions of different shear rates can coexist [31]. These effects are not included in any rheological theory and must be considered separately. For rheological measurements liquid failures are often an annoyance, but for elastohydrodynamics where the shear stress transferred across the film exhibits a plateau behavior just as banded flows do [31], the effect of liquid failure makes shear thinning at times appear to be a relatively insignificant part of the flow problem.

REFERENCES

[1] Bird RB, Armstrong RC, Hassager O. Dynamics of polymeric liquids. Volume 1: fluid mechanics: 2nd ed. A Wiley-Interscience Publication. New York: John Wiley & Sons; 1987 Jun. p. 1, 170-1,227-8, 351, 234, 174, 139.
[2] McCabe C, Cui S, Cummings PT, Gordon PA, Saeger RB. Examining the rheology of 9-octylheptadecane to giga-pascal pressures. J Chem Phys 2001;114(4):1887–91.
[3] Tanner RI. Engineering rheology. Oxford: Oxford Univ. Press; 2000. p. 55, 325, 18-19, 458–464.
[4] Currie IG. Fundamental mechanics of fluids. 2nd ed. New York: McGraw-Hill; 1993. p. 27.
[5] Barnes HA, Roberts GP. A simple empirical model describing the steady-state shear and extensional viscosities of polymer melts. J Non-Newton Fluid Mech 1992;44:113–26.
[6] Cross MM. Rheology of non-Newtonian fluids: a new flow equation for pseudo-plastic systems. J Colloid Sci 1965;20(5):417–37.
[7] Meter DM, Bird RB. Tube flow of non-Newtonian polymer solutions: Part I. laminar flow and rheological models. AIChE J 1964;10(6):878–81.
[8] Macosko CW. Rheology: principles, measurements, and applications. New York: VCH; 1994. p. 7.
[9] Williamson BP, Walters K, Bates TW, Coy RC, Milton AL. The viscoelastic properties of multigrade oils and their effect on journal-bearing characteristics. J Non-Newton Fluid Mech 1997;73(1-2):115–26.
[10] Keentok M, Georgescu AG, Sherwood AA, Tanner RI. The measurement of the second normal stress difference for some polymer solutions. J Non-Newton Fluid Mech 1980;6(3–4):303–24.
[11] De Kee D, Stastna J. Primary normal stress coefficient predictions. J Rheol 1986;30 (1):207–30.
[12] Binnington RJ, Boger DV. Constant viscosity elastic liquids. J Rheol 1985;29 (6):887–904.

[13] Joseph DD. Fluid dynamics of viscoelastic liquids. New York: Springer-Verlag; 1990. p. 11–3.
[14] Tevaarwerk J, Johnson KL. A simple non-linear constitutive equation for elastohydrodynamic oil films. Wear 1975;35(2):345–56.
[15] Schultheisz CR, Flynn KM, Leigh SD. Certification of the rheological behavior of SRM 2491, polydimethylsiloxane. NIST Special Publication, 260-147; 2001.
[16] Dyson A, Wilson AR. Film thickness in elastohydrodynamic lubrication by silicone fluids. Proc. Instn. Mech. Eng 1965–66;180(3):97–105.
[17] Harrison G. The dynamic properties of supercooled liquids. London and New York: Academic Press; 1976.
[18] Schultheisz CR, Leigh SD. Certification of the rheological behavior of SRM 2490, polyisobutylene dissolved in 2,6,10,14-tetramethylpentadecane. NIST Special Publication 260-143; 2002.
[19] Florez WF, Power H, Janna FC. Multi-domain dual reciprocity for the solution of inelastic non-Newtonian flow problems at low Reynolds number. Computat Mech 2001;27(5):396–411.
[20] Van Krevelen DW, Te Nijenhuis K. Properties of polymers: their correlation with chemical structure; their numerical estimation and prediction. 3rd ed. Amsterdam: Elsevier; 1990. p. 477.
[21] Rotem Z. Non-Newtonian flow in annuli. J Appl Mech 1962;29(2):421–4.
[22] Carreau PJ. Rheological equations from molecular network theories. Transact Soc Rheol 1972;16(1):99–127.
[23] Bair S, Khonsari M. An EHD inlet zone analysis incorporating the second Newtonian. J Tribol. 1996;118(2):341–3.
[24] Bair S. A rough shear-thinning correction for EHD film thickness. Tribol Transact 2004;47(3):361–5.
[25] Ree F, Ree T, Eyring H. Relaxation theory of transport problems in condensed systems. Indust Eng Chem 1958;50(7):1036–40.
[26] Schurz J, Vollrath-Rodiger M, Krassig H. Rheologische Untersuchungen an Polacrylnitril-Spinnlosungen: Erweiterung HV 6 fur hohere Temperaturen. Rheol Acta 1981;20:569–78.
[27] Bird RB, Curtiss C, Armstrong R, Hassager O. Dynamics of polymer liquids vol. 2 Kinetic theory. 2nd ed. New York: Wiley; 1987.
[28] Hutton JF. Theory of rheology. In: Ku PM, editor. Interdisciplinary approach to liquid lubricant technology. Washington: NASA; 1973. p. 187–261.
[29] Fisher JC. The fracture of liquids. J Appl Phys 1948;19(11):1062–7.
[30] Kottke PA, Bair SS, Winer WO. Cavitation in creeping shear flows. AIChE J 2005;51(8):2150–70.
[31] Lee JY, Fuller GG, Hudson NE, Yuan XF. Investigation of shear-banding structure in wormlike micellar solution by point-wise flow-induced birefringence measurements. J Rheol 2005;49(2):537–50.